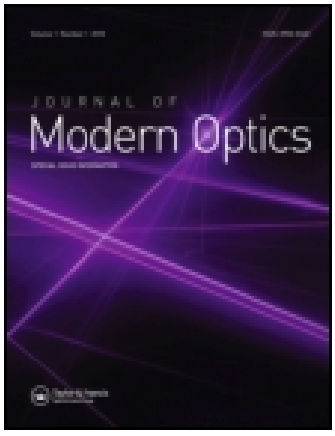

Journal of Modern Optics
Publication details, including instructions for authors and subscription information:
http://www.tandfonline.com/loi/tmop20

The frequency crossover for the Goos-Hänchen shift

Manoel P. Araújo[a], Silvânia A. Carvalho[b] & Stefano De Leo[b]
[a] Gleb Wataghin Physics Institute, State University of Campinas, Campinas, Brazil
[b] Department of Applied Mathematics, State University of Campinas, Campinas, Brazil
Published online: 04 Dec 2013.

To cite this article: Manoel P. Araújo, Silvânia A. Carvalho & Stefano De Leo (2013) The frequency crossover for the Goos-Hänchen shift, Journal of Modern Optics, 60:20, 1772-1780, DOI: 10.1080/09500340.2013.860199

To link to this article: http://dx.doi.org/10.1080/09500340.2013.860199

Journal of Modern Optics, 2013
Vol. 60, No. 20, 1772–1780, http://dx.doi.org/10.1080/09500340.2013.860199

Taylor & Francis
Taylor & Francis Group

The frequency crossover for the Goos–Hänchen shift

Manoel P. Araújo[a], Silvânia A. Carvalho[b]*, Stefano De Leo[b]

[a] *Gleb Wataghin Physics Institute, State University of Campinas, Campinas, Brazil;* [b] *Department of Applied Mathematics, State University of Campinas, Campinas, Brazil*

(*Received 11 July 2013; accepted 24 October 2013*)

For total reflection, the Goos–Hänchen (GH) shift is proportional to the wavelength of the laser beam. At critical angles, such a shift is instead proportional to the square root of the product of the beam waist and wavelength. By using the stationary phase method (SPM) and, when necessary, numerical calculations, we present a detailed analysis of the frequency crossover for the GH shift. The study, done in different incidence regions, sheds new light on the validity of the analytic formulas found in literature.

Keywords: Goos–Hänchen shift; stationary phase method; wavenumber distribution

1. Introduction

The GH shift, widely investigated in the last few decades, continues to attract attention due to available technologies [1–12]. This phenomenon refers to the lateral shift of a totally reflected beam with respect to the optical path expected from geometrical optics. For an interesting overview of the effect and its generalizations, we suggest the references [11,12]. The fact that total reflection does not take place at the spatial point predicted by the geometrical optics, see Figure 1(*a*), was discovered by Newton [13] who proposed that the path during total reflection is a parabola, the vertex being within the rarer medium. The problem was then experimentally and theoretically analyzed by other authors in 1920s and 1930s [14,15]. The first experimental observation of this effect was done by Goos and Hänchen [16]. Their experiment stimulated the study of this shift for different polarized electromagnetic waves [17,18]. In the literature, the longitudinal and transverse shifts of an optical beam have been investigated by using the far-field measurement for the reflected field and the scanning tunneling optical microscope for the (evanescent) transmitted beam [1].

The fact that the GH shift has been investigated in different physical problems, see frustrated total internal reflection (FTIR) [19–21], partial reflection [22], acoustic [23], nonlinear optics [24], frequency dispersive media [25,26], and surface physics [27], shows the great and increasing attention of the scientific community to this topic. Some interesting applications, which include sensors and optical waveguide switching, can be found in recent research works [9,28–30]. On the other hand, the measurement of this very small shift (of the order of the beam wavelength) represented a continuous challenge. The proposed solutions to increase its magnitude were discussed in many works [8,31,32]. Over the years, this technical problem was solved and it is now possible to measure this shift [33].

In 1948, Artmann obtained an expression for the GH shift at critical angle [17]. After a few decades, other authors studied the same problem in detail obtaining an expression for the lateral shift for incidence angles very close to the critical angle [34–36].

In this paper, we describe the beam propagation into the dielectric block by using the analogy between optcis and quantum mechanics [37,38]. In particular, we derive the transmission and reflection coefficients at each interface and then calculate both analytically and numerically the position of the outgoing beam. The wave packet formalism is introduced by considering a gaussian wave number distribution. The SPM, applied to our gaussian beams, leads to an analytical formula for the exit point of the optical beam propagating throughout a right angle prism with refractive index n [39–41]. The difference between the geometrical result obtained by the Snell law and the real optical path and its frequency crossover will be the subject of our investigation.

The study done in this paper allows one to investigate the validity of the analytical formulas for different incidence angles as well the transition from partial to total internal reflection. A new formula, based on the SPM, is presented for the shift at critical incidence. The numerical analysis confirms our analytical predictions.

*Corresponding author. Email: silalves@ime.unicamp.br

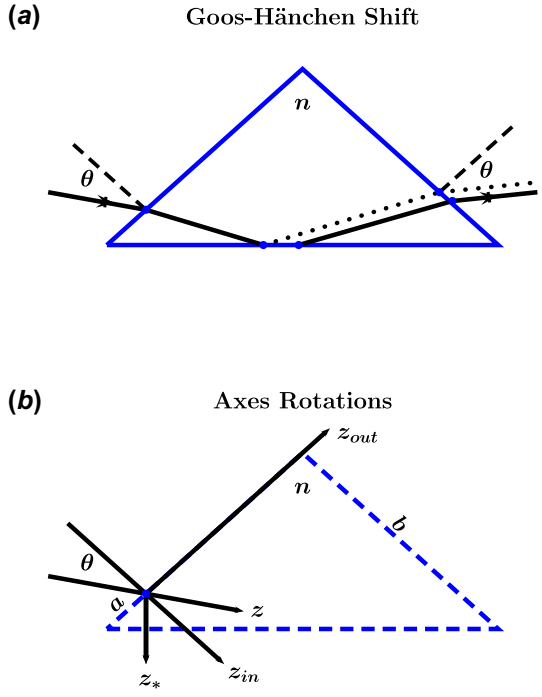

Figure 1. Schematic diagram of the dielectric block analyzed in this paper. In (*a*), the lateral displacement (solid line) of the reflected beam at the down dielectric–air interface with respect to geometrical path (dotted line) is shown. In (*b*), we draw the axes of the incoming propagation, z, and of the normal to the left air/dielectric boundary, $z_{\rm in}$, to the down dielectric/air boundary, z_*, and to the right air/dielectric boundary, $z_{\rm out}$. (The color version of this figure is included in the online version of the journal.)

This paper is organized as follows. In the following section, we discuss the Gaussian beam propagation in free space. The geometry of the physical system is presented in Section 3. In Section 4, we calculate, by using the analogy between optics and quantum mechanics, the reflection and transmission coefficients for s and p polarized waves [42]. In Section 5, by using the SPM, we analyze the quantum additional phase and give our analytical expressions for the GH shift for different incidence regions. The numerical results are then presented in Section 6. Our conclusions and proposals for future investigations are drawn in the final section.

2. The incoming Gaussian beam

The beam propagation in free space is determined by the wave number laser distribution [43]. Let us consider the following distribution,

$$G(\boldsymbol{k}) = \exp\left[-\frac{(k_x^2+k_y^2)w_0^2}{4}\right]\delta\left(k_z-\left(k^2-k_x^2-k_y^2\right)^{1/2}\right), \tag{1}$$

where w_0 is the beam waist size and $k=2\pi/\lambda$. The electric field amplitude is then given by

$$\begin{aligned} E_{\rm in}(\boldsymbol{r}) &= E_0\frac{w_0^2}{4\pi}\int {\rm d}\boldsymbol{k}G(\boldsymbol{k})\exp\left[{\rm i}\boldsymbol{k}\cdot\boldsymbol{r}\right] \\ &= E_0\frac{w_0^2}{4\pi}\int {\rm d}k_x{\rm d}k_y\exp\left[-\frac{(k_x^2+k_y^2)w_0^2}{4}\right] \\ &\quad\times\exp\left[{\rm i}\left(k_xx+k_yy+\left(k^2-k_x^2-k_y^2\right)^{1/2}z\right)\right], \end{aligned} \tag{2}$$

with $E_0=E(\boldsymbol{0})$. By considering the paraxial approximation (valid for $kw_0\geq 5$), the integrations can be done analytically leading to

$$\begin{aligned} E_{\rm in}(\boldsymbol{r}) &\approx E_0\frac{w_0^2}{4\pi}\exp({\rm i}kz)\int {\rm d}k_x{\rm d}k_y\exp\left[-\frac{(k_x^2+k_y^2)w_0^2}{4}\right] \\ &\quad\times\exp\left[{\rm i}\left(k_xx+k_yy-\frac{k_x^2+k_y^2}{2k}z\right)\right] \\ &\approx E_0\frac{w_0^2}{w_0^2+2{\rm i}(z/k)}\exp({\rm i}kz)\exp\left[-\frac{x^2+y^2}{w_0^2+2{\rm i}(z/k)}\right]. \end{aligned} \tag{3}$$

The intensity, $I(\boldsymbol{r})=|E(\boldsymbol{r})|^2$, for the incoming beam is then given by

$$I_{\rm in}(\boldsymbol{r})\approx {\rm I}_0\left[\frac{w_0}{w(z)}\right]^2\exp\left[-2\frac{x^2+y^2}{w^2(z)}\right], \tag{4}$$

where

$$w(z)=w_0\left[1+\left(\frac{\lambda z}{\pi w_0^2}\right)^2\right]^{1/2}.$$

3. The spatial phase of the outgoing beam

In this section, we determine the direction of propagation of the outgoing beam by calculating its spatial phase. In doing this, it is convenient to introduce new axes of coordinates, see Figure 1(*b*). The plane of incidence is the y–z plane, where z is the propagation direction of the incoming beam, and the new axes represent rotation of the y–z system with $z_{\rm in}$, z_*, and $z_{\rm out}$ normal to the left (air/dielectric), down (dielectric/air) and right (dielectric/air) interface. Denoting the incidence angle by θ and using $R(\theta)$ to identify a counterclockwise,

$$R(\theta)=\begin{pmatrix}\cos\theta & -\sin\theta\\ \sin\theta & \cos\theta\end{pmatrix},$$

we find

$$\begin{aligned} \begin{pmatrix}y_{\rm out}\\ z_{\rm out}\end{pmatrix} &= R\left(\frac{3\pi}{4}\right)\begin{pmatrix}y_*\\ z_*\end{pmatrix} = R\left(\frac{\pi}{2}\right)\begin{pmatrix}y_{\rm in}\\ z_{\rm in}\end{pmatrix} \\ &= R\left(\frac{\pi}{2}-\theta\right)\begin{pmatrix}y\\ z\end{pmatrix}. \end{aligned} \tag{5}$$

The spatial phase of the incoming beam is

$$\varphi_{\text{in}} = \boldsymbol{k} \cdot \boldsymbol{r} = \boldsymbol{k}_{\text{in}} \cdot \boldsymbol{r}_{\text{in}}, \tag{6}$$

where $\boldsymbol{r}_{\text{in}} = (x, y_{\text{in}}, z_{\text{in}})$ is obtained from Equation (5) and $\boldsymbol{k}_{\text{in}}$ is given by

$$k_{x_{\text{in}}} = k_x \text{ and } \begin{pmatrix} k_{y_{\text{in}}} \\ k_{z_{\text{in}}} \end{pmatrix} = R(-\theta) \begin{pmatrix} k_y \\ k_z \end{pmatrix}. \tag{7}$$

Taking into account that the discontinuity is along the z_{in} axis, the $x_{\text{in}}(= x)$ and y_{in} components of the wave number do not change when the beam crosses the first air/dielectric boundary,

$$(q_x, q_{y_{\text{in}}}) = (k_x, k_{y_{\text{in}}}) \Rightarrow q_{z_{\text{in}}} = \left(n^2 k^2 - k_x^2 - k_{y_{\text{in}}}^2\right)^{1/2}. \tag{8}$$

The spatial phase of the beam moving in the dielectric from the left (air/dielectric) to the down (dielectric/air) interface is

$$\varphi_{\text{left/down}} = \boldsymbol{q}_{\text{in}} \cdot \boldsymbol{r}_{\text{in}} = \boldsymbol{q}_* \cdot \boldsymbol{r}_*, \tag{9}$$

where $\boldsymbol{r}_* = (x, y_*, z_*)$ is obtained from Equation (5) and $\boldsymbol{q}_*$ is given by

$$q_{x_*} = k_x \text{ and } \begin{pmatrix} q_{y_*} \\ q_{z_*} \end{pmatrix} = R\left(-\frac{\pi}{4}\right) \begin{pmatrix} q_{y_{\text{in}}} \\ q_{z_{\text{in}}} \end{pmatrix}. \tag{10}$$

The spatial phase of the reflected beam at the down interface is obtained from Equation (9) by changing z_* in $-z_*$,

$$\varphi_{\text{down/right}} = q_{x_*} x_* + q_{y_*} y_* - q_{z_*} z_* = \boldsymbol{q}_{\text{out}} \cdot \boldsymbol{r}_{\text{out}}, \tag{11}$$

where $\boldsymbol{r}_{\text{out}} = (x, y_{\text{out}}, z_{\text{out}})$ is obtained from Equation (5) and $\boldsymbol{q}_{\text{out}}$ is given by

$$q_{x_{\text{out}}} = k_x \text{ and } \begin{pmatrix} q_{y_{\text{out}}} \\ q_{z_{\text{out}}} \end{pmatrix} = R\left(\frac{3\pi}{4}\right) \begin{pmatrix} q_{y_*} \\ -q_{z_*} \end{pmatrix} = \begin{pmatrix} -q_{y_{\text{in}}} \\ q_{z_{\text{in}}} \end{pmatrix}. \tag{12}$$

The beam reaches the right (dielectric/air) boundary and due to the fact that the discontinuity is along the z_* axis, the $x_*(= x)$ and y_* components of the wave number do not change when the beam crosses the last dielectric/air interface,

$$\begin{aligned}(k_x, k_{y_{\text{out}}}) = (k_x, q_{y_{\text{out}}}) = (k_x, -q_{y_{\text{in}}}) = (k_x, -k_{y_{\text{in}}}) \\ \Rightarrow k_{z_{\text{out}}} = k_{z_{\text{in}}}.\end{aligned} \tag{13}$$

Finally, the spatial phase of the outgoing beam is

$$\begin{aligned}\varphi_{\text{out}} = \boldsymbol{k}_{\text{out}} \cdot \boldsymbol{r}_{\text{out}} &= k_x x - k_{y_{\text{in}}} y_{\text{out}} + k_{z_{\text{in}}} z_{\text{out}} \\ &= k_x x + (k_z \cos 2\theta - k_y \sin 2\theta) y \\ &\quad + (k_z \sin 2\theta + k_y \cos 2\theta) z.\end{aligned} \tag{14}$$

Consequently, the outgoing wave number vector in the (x, y, z) coordinates system is given by

$$\begin{aligned}[\nabla \varphi_{\text{out}}]_{(k_x=0, k_y=0)} &= (0, k \cos 2\theta, k \sin 2\theta) \\ &\quad \times \begin{cases} (0, 0, k) & \text{for } \theta = \pi/4, \\ (0, k, 0) & \text{for } \theta = 0, \\ (0, 0, -k) & \text{for } \theta = -\pi/4. \end{cases}\end{aligned} \tag{15}$$

The outgoing beam propagates parallel to the incoming beam for $\theta = \pm\pi/4$ and perpendicular to the incoming beam for $\theta = 0$.

4. Transmission coefficient and geometrical path

The Fresnel formulas for the reflection and transmission coefficients of s-polarized beam can be given by using the analogy between optics and quantum mechanics [41]. From the non-relativistic quantum analysis of the step potential [42],

$$r[\alpha, \beta] = \frac{\alpha - \beta}{\alpha + \beta} \quad \text{and} \quad t[\alpha, \beta] = \frac{2\alpha}{\alpha + \beta}, \tag{16}$$

we find

$$\begin{aligned} r_{\text{in}}^{(s)} &= r[k_{z_{\text{in}}}, q_{z_{\text{in}}}] \exp[2\mathrm{i} k_{z_{\text{in}}} a_{\text{in}}], \\ t_{\text{in}}^{(s)} &= t[k_{z_{\text{in}}}, q_{z_{\text{in}}}] \exp[\mathrm{i}(k_{z_{\text{in}}} - q_{z_{\text{in}}}) a_{\text{in}}], \\ r_*^{(s)} &= r[q_{z_*}, k_{z_*}] \exp[2\mathrm{i} q_{z_*} a_*], \\ t_*^{(s)} &= t[q_{z_*}, k_{z_*}] \exp[\mathrm{i}(q_{z_*} - k_{z_*}) a_*], \\ r_{\text{out}}^{(s)} &= r[q_{z_{\text{out}}}, k_{z_{\text{out}}}] \exp[2\mathrm{i} q_{z_{\text{out}}} a_{\text{out}}], \\ t_*^{(s)} &= t[q_{z_{\text{out}}}, k_{z_{\text{out}}}] \exp[\mathrm{i}(q_{z_{\text{out}}} - k_{z_{\text{out}}}) a_{\text{out}}]. \end{aligned} \tag{17}$$

By choosing the axes origin in $a_{\text{in}} = 0$ (this implies $a_* = a/2^{1/2}$ and $a_{\text{out}} = b - a$) and observing that $q_{z_{\text{out}}} = q_{z_{\text{in}}}$ and $k_{z_{\text{out}}} = k_{z_{\text{in}}}$, we obtain the following expression for the transmission coefficient

$$t^{(s)} = t_{\text{in}}^{(s)} r_*^{(s)} t_{\text{out}}^{(s)} = \frac{4 k_{z_{\text{in}}} q_{z_{\text{in}}}}{(k_{z_{\text{in}}} + q_{z_{\text{in}}})^2} \frac{q_{z_*} - k_{z_*}}{q_{z_*} + k_{z_*}} \exp[\mathrm{i}\psi_{\text{out}}], \tag{18}$$

where

$$\psi_{\text{out}} = q_{z_*} a\, 2^{1/2} + (q_{z_{\text{in}}} - k_{z_{\text{in}}})(b - a). \tag{19}$$

The transmission coefficient for p-polarized is found by the substitution rule

$$(k_{z_{\text{in},*}}, q_{z_{\text{in},*}}) \to \left(n k_{z_{\text{in},*}}, \frac{q_{z_{\text{in},*}}}{n}\right),$$

in

$$\frac{4 k_{z_{\text{in}}} q_{z_{\text{in}}}}{(k_{z_{\text{in}}} + q_{z_{\text{in}}})^2} \frac{q_{z_*} - k_{z_*}}{q_{z_*} + k_{z_*}}.$$

This leads to

$$t^{(p)} = \frac{4 n^2 k_{z_{\text{in}}} q_{z_{\text{in}}}}{(n^2 k_{z_{\text{in}}} + q_{z_{\text{in}}})^2} \frac{q_{z_*} - n^2 k_{z_*}}{q_{z_*} + n^2 k_{z_*}} \exp[\mathrm{i}\psi_{\text{out}}]. \tag{20}$$

Once the transmission coefficient is obtained, we can write, by using a gaussian convolution, the amplitude of the outgoing electric field [41],

$$\begin{aligned} E_{\text{out}}^{(s,p)}(\boldsymbol{r}) = E_0 \frac{w_0^2}{4\pi} \int \mathrm{d}k_x \mathrm{d}k_y t^{(s,p)} \exp\left[-\frac{(k_x^2 + k_y^2) w_0^2}{4}\right] \\ \times \exp\left[\mathrm{i}\boldsymbol{k}_{\text{out}} \cdot \boldsymbol{r}_{\text{out}}\right]. \end{aligned} \tag{21}$$

Now the geometrical path can be calculated by using the SPM [39–41]. To illustrate the method, let us consider the

incoming beam. By imposing that the derivative of the phase is zero at the center of our symmetric gaussian distribution, we immediately find

$$\left[\frac{\partial\varphi_{\rm in}}{\partial k_x},\frac{\partial\varphi_{\rm in}}{\partial k_y}\right]_{(k_x=0,k_y=0)}=(0,0)\Rightarrow(x_{\rm max},y_{\rm max})_{\rm in}=(0,0). \quad (22)$$

For the outgoing beam, the phase is given by the spatial phase $\varphi_{\rm out}$ and by the phase $\psi_{\rm out}$ coming from the transmission coefficient. By using the SPM, we find

$$\left[\frac{\partial(\varphi_{\rm out}+\psi_{\rm out})}{\partial k_x}\right]_{(0,0)}=0\Rightarrow x_{\rm max,out}=0, \quad (23)$$

and

$$\left[\frac{\partial(\varphi_{\rm out}+\psi_{\rm out})}{\partial k_y}\right]_{(0,0)}=0\Rightarrow z_{\rm max}\cos 2\theta-y_{\rm max}\sin 2\theta=d, \quad (24)$$

where

$$d=a(\cos\theta+\sin\theta)+b\sin\theta\left(\frac{\cos\theta}{\left(n^2-\sin^2\theta\right)^{1/2}}-1\right). \quad (25)$$

For refractive index $n=2^{1/2}$, we can observe the output beam maximum moving along

$$\begin{aligned} y&=\frac{b}{2^{1/2}}\left(1-\frac{1}{(2n^2-1)^{1/2}}\right)-a\,2^{1/2} && \text{for } \theta=\pi/4,\\ z&=a && \text{for } \theta=0,\\ y&=\frac{b}{2^{1/2}}\left(1-\frac{1}{(2n^2-1)^{1/2}}\right) && \text{for } \theta=-\pi/4. \end{aligned} \quad (26)$$

For $\theta=\pi/4$, the choice of

$$a=\frac{(2n^2-1)^{1/2}-1}{2(2n^2-1)^{1/2}}b,$$

implies $y=0$. Consequently the incoming and outgoing beams move in the same direction.

5. The Goos–Hänchen shift by the SPM

The optical path obtained in the previous section by using the SPM can also be determined by applying the Snell law. In this section, we present the calculation of the additional quantum phase which cannot be predicted by geometrical optics. At the down interface, the reflection coefficients for s and p polarized wave are

$$\left\{r_*^{(s)},r_*^{(p)}\right\}=\left\{\frac{q_{z*}-k_{z*}}{q_{z*}+k_{z*}},\frac{q_{z*}-n^2k_{z*}}{q_{z*}+n^2k_{z*}}\right\}\exp[2{\rm i}q_{z*}a_*].$$

Let us expand k_{z*} around the center of the gaussian wave number distribution, i.e. $k_x=k_y=0$,

$$\begin{aligned} k_{z*}^2(k_x,k_y)&=k_{z*}^2(0,0)+\left[\frac{\partial k_{z*}^2}{\partial k_y}\right]_{(0,0)}k_y+O[k_x^2,k_y^2]\\ &=k_{z*}^2(0,0)+2q_{z*}(0,0)\left[\frac{\partial q_{z*}}{\partial k_y}\right]_{(0,0)}k_y\\ &\quad+O[k_x^2,k_y^2]. \end{aligned} \quad (27)$$

By using

$$k_{z*}^2(0,0)=-\frac{k^2}{2}\left(n^2-2+2\sin\theta\left(n^2-\sin^2\theta\right)^{1/2}\right),$$

$$q_{z*}(0,0)=\frac{k}{2^{1/2}}\left(-\sin\theta+\left(n^2-\sin^2\theta\right)^{1/2}\right)^{1/2},$$

and

$$\left[\frac{\partial q_{z*}}{\partial k_y}\right]_{(0,0)}=-\frac{\cos\theta}{2^{1/2}}\left(1+\frac{\sin\theta}{\left(n^2-\sin^2\theta\right)^{1/2}}\right),$$

we obtain

$$\frac{k_{z*}^2(k_x,k_y)}{k^2}=\left(1-\frac{n^2}{2}-\sin\theta\left(n^2-\sin^2\theta\right)^{1/2}\right)-\frac{\cos\theta(n^2-2\sin^2\theta)}{\left(n^2-\sin^2\theta\right)^{1/2}}\frac{k_y}{k}. \quad (28)$$

For $k_y>\sigma(n,\theta)k$,

$$\sigma(n,\theta)=\frac{\left(1-\frac{n^2}{2}-\sin\theta\left(n^2-\sin^2\theta\right)^{1/2}\right)\left(n^2-\sin^2\theta\right)^{1/2}}{\cos\theta\left(n^2-2\sin^2\theta\right)}, \quad (29)$$

we have $k_{z*}^2<0$ and consequently an additional quantum phase has to be considered in calculating the optical path,

$$\begin{aligned} \left\{\widetilde{\psi}_{\rm out}^{(s)},\widetilde{\psi}_{\rm out}^{(p)}\right\}&=\left\{{\rm Arg}\left[\frac{q_{z*}-{\rm i}\,|k_{z*}|}{q_{z*}+{\rm i}\,|k_{z*}|}\right],{\rm Arg}\left[\frac{q_{z*}-{\rm i}n^2|k_{z*}|}{q_{z*}+{\rm i}n^2|k_{z*}|}\right]\right\}\\ &=-2\left\{\arctan\left[\frac{|k_{z*}|}{q_{z*}}\right],\arctan\left[\frac{n^2|k_{z*}|}{q_{z*}}\right]\right\}. \end{aligned} \quad (30)$$

The derivatives of these phases,

$$\left\{\frac{\partial\widetilde{\psi}_{\rm out}^{(s)}}{\partial k_y},\frac{\partial\widetilde{\psi}_{\rm out}^{(p)}}{\partial k_y}\right\}=\frac{2}{|k_{z*}|}\frac{\partial q_{z*}}{\partial k_y}\left\{1,\frac{n^2k^2}{k^2+(n^2+1)|k_{z*}|^2}\right\}, \quad (31)$$

will be then used to obtain the GH shift. To determine at which k_y-value the previous derivatives have to be calculated, we analyze the wave number distribution for different incidence angle, see Figure 2. For $\sigma(2^{1/2},\theta)kw_0\le-5$ (Figure 2(*a*)), the wave packet is totally reflected and its wave number distribution is a symmetric distribution. Thus,

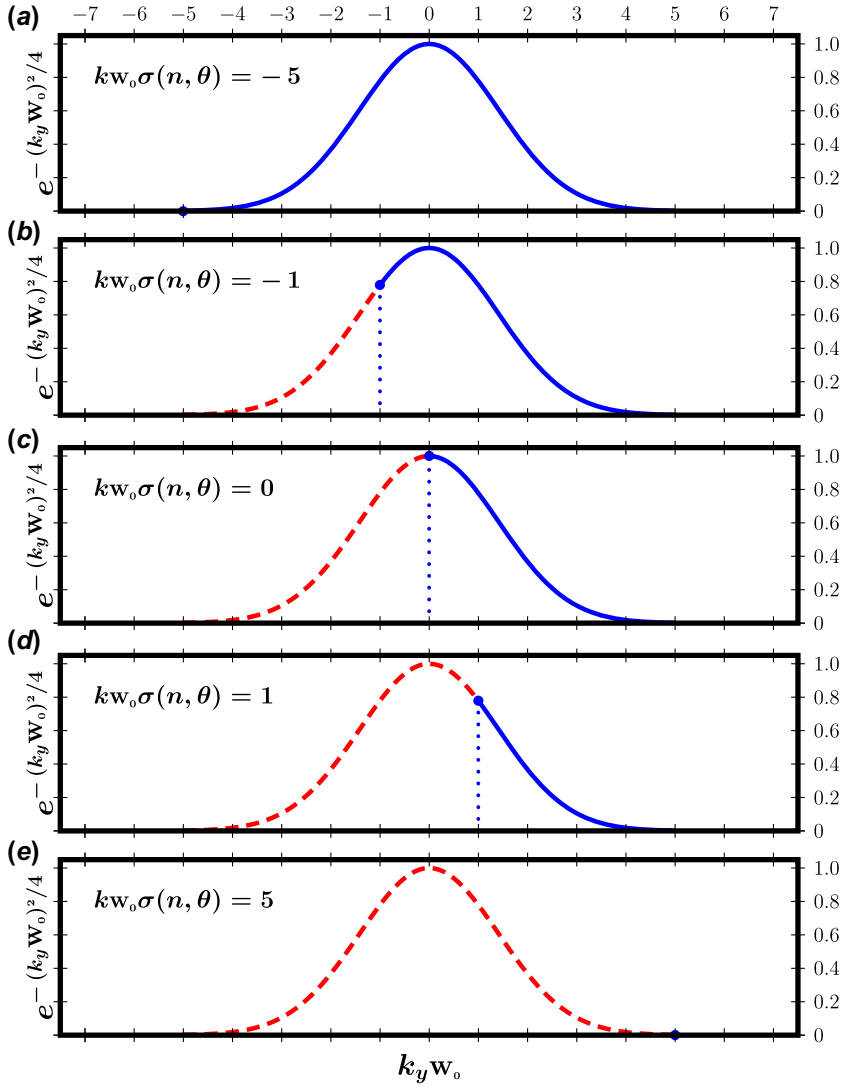

Figure 2. Gaussian wave number distribution for different incidence angles. The dotted line represents the part of the distribution with a real reflection coefficient, $k_{z*}^2 > 0$. The solid line represents the part of the distribution with a complex reflection coefficient, $k_{z*}^2 < 0$. (The color version of this figure is included in the online version of the journal.)

the derivative of additional phase must be calculated at its center, $k_y = 0$. For $\sigma(2^{1/2}, \theta)kw_0 \leq 5$ (Figure 2(*e*)), the reflection coefficient is real and there is not an additional phase. The intermediate case, $\sigma(2^{1/2}, \theta)kw_0 = 0$ (Figure 2(*c*)), represents incidence at the critical angle. In this case, only a half part of the wave number distribution contains an additional phase. Consequently, the derivatives have to be calculated at $k_y = k_c$,

$$k_c = \frac{\int_0^{+\infty} \mathrm{d}k_y k_y \exp\left[-(k_y w_0)^2/2\right]}{\int_{-\infty}^{+\infty} \mathrm{d}k_y \exp\left[-(k_y w_0)^2/2\right]} = \frac{1}{(2\pi)^{1/2} w_0}. \quad (32)$$

- $\sigma(n, \theta)kw_0 \leq -5$

In this case, we have to calculate the derivatives in $(k_x, k_y) = (0, 0)$. We find

$$\left\{\frac{\partial \widetilde{\psi}_{\mathrm{out}}^{(s)}}{\partial k_y}, \frac{\partial \widetilde{\psi}_{\mathrm{out}}^{(p)}}{\partial k_y}\right\}_{(0,0)} = -\left\{\widetilde{d}_T^{(s)}, \widetilde{d}_T^{(p)}\right\}, \quad (33)$$

with

$$\widetilde{d}_T^{(s)} = \frac{2\cos\theta}{k\left(n^2 - 2 + 2\sin\theta\left(n^2 - \sin^2\theta\right)^{1/2}\right)^{1/2}} \times \left(1 + \frac{\sin\theta}{\left(n^2 - \sin^2\theta\right)^{1/2}}\right),$$

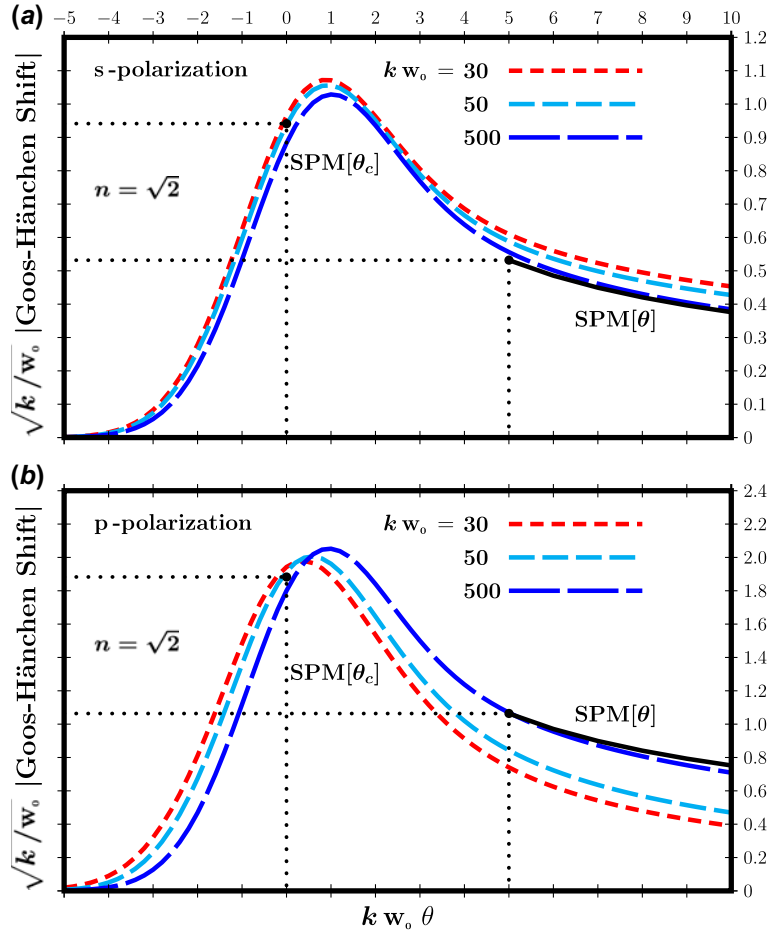

Figure 3. The numerical GH shift is plotted as a function of the incidence angle for a fixed refractive index, $n = 2^{1/2}$, and three different values of kw_0 (dashed lines). The numerical data are in excellent agreement with our analytical predictions for the GH shift, $\widetilde{d}_C^{(s,p)}$ (dot) and $\widetilde{d}_T^{(s,p)}$ (solid line for $kw_0 = 500$). (The color version of this figure is included in the online version of the journal.)

$$\widetilde{d}_T^{(p)} = \frac{n^2}{1 + (n^2+1)\left(\frac{n^2}{2} - 1 + \sin\theta\left(n^2 - \sin^2\theta\right)^{1/2}\right)}\widetilde{d}_T^{(s)}. \tag{34}$$

- $\sigma(n,\theta)kw_0 = 0$

For incidence at critical angle, we have to calculate the derivatives in $(k_x, k_y) = (0, k_c)$, i.e.

$$\left\{\frac{\partial\widetilde{\psi}_{\text{out}}^{(s)}}{\partial k_y}, \frac{\partial\widetilde{\psi}_{\text{out}}^{(p)}}{\partial k_y}\right\}_{(0,k_c)} = \frac{2}{|k_{z_*}(0,k_c)|}\left[\frac{\partial q_{z_*}}{\partial k_y}\right]_{(0,k_c)} \times \left\{1, \frac{n^2k^2}{k^2 + (n^2+1)|k_{z_*}(0,k_c)|^2}\right\}. \tag{35}$$

Recalling that at critical angles $k_{z_*}(0,0) = 0$, by using Equation (27),

$$k_{z_*}^2\left(0, \langle k_y\rangle\right) \approx 2k\left(n^2-1\right)^{1/2}\left[\frac{\partial q_{z_*}}{\partial k_y}\right]_{(0,0)}\langle k_y\rangle \tag{36}$$

and observing that

$$\left[\frac{\partial q_{z_*}}{\partial k_y}\right]_{(0,k_c)} \approx \left[\frac{\partial q_{z_*}}{\partial k_y}\right]_{(0,0)}, \tag{37}$$

we get

$$\left\{\frac{\partial\widetilde{\psi}_{\text{out}}^{(s)}}{\partial k_y}, \frac{\partial\widetilde{\psi}_{\text{out}}^{(p)}}{\partial k_y}\right\}_{(0,k_c)} = -\left\{\widetilde{d}_C^{(s)}, \widetilde{d}_C^{(p)}\right\}, \tag{38}$$

with

$$\widetilde{d}_C^{(s)} = 2^{1/2}\frac{(kw_0)^{1/2}}{k}\left[\frac{\pi}{(n^2-1)}\right]^{1/4} \times \left(\cos\theta_C\left(1 + \frac{\sin\theta_C}{\left(n^2 - \sin^2\theta_C\right)^{1/2}}\right)\right)^{1/2},$$

$$\widetilde{d}_C^{(p)} = n^2\widetilde{d}_C^{(s)}. \tag{39}$$

The analytical formulas obtained for the GH shift will be tested in the next section by a numerical analysis.

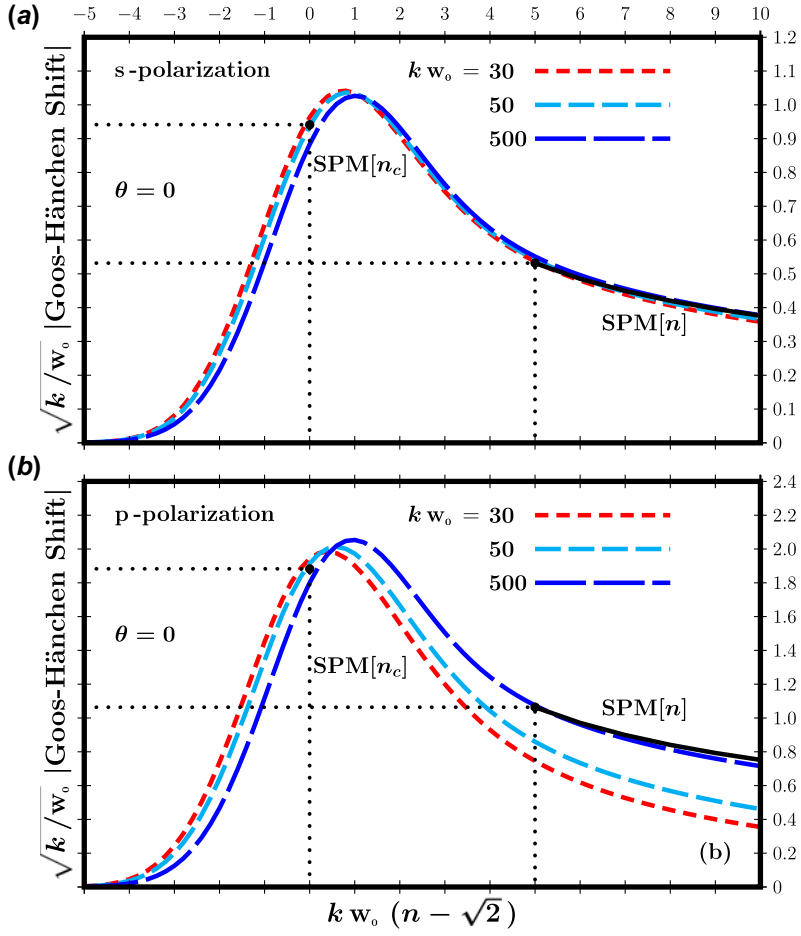

Figure 4. The numerical GH shift is plotted as a function of the refractive index for a fixed incidence angle, $\theta = 0$, and three different values of kw_0 (dashed lines). The numerical data are in excellent agreement with our analytical predictions for the GH shift, $\widetilde{d}_C^{(s,p)}$ (dot) and $\widetilde{d}_T^{(s,p)}$ (solid line for $kw_0 = 500$). (The color version of this figure is included in the online version of the journal.)

6. Numerical analysis

In this section, we present a numerical analysis of the GH shift for gaussian optical beams. The intensity of the outgoing beam is given by

$$I_{\rm out}(\boldsymbol{r}) = |E_{\rm out}(\boldsymbol{r})|^2 \qquad (40)$$
$$= I_0 \left| \frac{w_0^2}{4\pi} \int {\rm d}k_x {\rm d}k_y \left| t^{(s,p)} \right| \exp\left[-\frac{(k_x^2+k_y^2)w_0^2}{4} + {\rm i}\left(\boldsymbol{k}_{\rm out}\cdot\boldsymbol{r}_{\rm out} + \psi_{\rm out} + \widetilde{\psi}_{\rm out}^{(s,p)} \right) \right] \right|^2 .$$

To estimate the GH shift, we calculate the deviation from the geometrical maximum,

$$z_{\max}\cos 2\theta - y_{\max}\sin 2\theta = d,$$

given in Section 4 (and also obtained from the Snell law). In Figure 3, we plot the numerical data corresponding to the GH shift, for s and p polarized waves, obtained for a fixed refractive index, $n = 2^{1/2}$, by varying the incidence angle and $kw_0 (= 30, 50, 500)$. In Figure 4, the plots refer to a fixed incidence angle, $\theta = 0$, and a varying refractive index. The numerical analysis shows an excellent agreement with our analytical prediction for the shift at critical angles. Observe that

$$\left(\frac{k}{w_0}\right)^{1/2} \widetilde{d}_C^{(s,p)}$$

only depends on the refractive index n (note that θ_c can be expressed as a function of n), see Equations (39).

For $\sigma(n,\theta)kw_0 \le -5$, we have to use for the GH shift the analytical expressions given in Equations (34). Now,

$$\left(\frac{k}{w_0}\right)^{1/2} \widetilde{d}_T^{(s,p)}$$

is proportional to $1/(kw_0)^{1/2}$ (in Figures 3 and 4, we have used $kw_0 = 500$ for the analytical curve). For a fixed refractive index, say $n = 2^{1/2}$,

$$\sigma(2^{1/2},\theta)kw_0 \le -5 \Rightarrow \tan\theta \frac{2-\sin^2\theta}{2\cos^2\theta} \ge \frac{5}{kw_0}.$$

For such angles, we can use our analytical expression which shows an excellent agreement with the numerical data, see Figure 3. For a fixed incidence angle, say $\theta = 0$,

$$\sigma(n, 0)kw_0 \leq -5 \Rightarrow \frac{n^2 - 2}{2n} \geq \frac{5}{kw_0}.$$

For such refractive indexes, the analytical expression shows an excellent agreement with the numerical data, see Figure 4. We conclude this section, by observing that the numerical data confirms a maximum GH shift for incidence angles *greater* than the critical ones [34].

7. Conclusions

In this paper, we have discussed the frequency crossover for the GH shift. The analytical formulas obtained by the SPM have then been numerically tested. Our study sheds new light on the validity region of the analytical formulas and on the transition region between partial and total reflection. The geometrical optical path derived by the SPM in Section 4 can also be obtained by the Snell law in geometrical optics. Nevertheless, the GH shift cannot be predicted by geometrical optics. For the calculation of an analytical formula for this shift, the use of the SPM is not a matter of taste. It is important to observe that, for total reflection, our wave number distributions are symmetric and consequently the derivatives have to be calculated at their center, located at $k_y = 0$. This leads to a shift of the order of $\lambda/2\pi = c/\omega$.

In our analysis, the SPM has been extended to the critical regime. The formula for critical incidence has been obtained by calculating the derivatives at $k_y = k_c$, see Equation (32). This is due to the fact that for incidence at critical angles the wave number distribution is not symmetric. The GH shift is now amplified by the factor $(kw_0)^{1/2}$.

The numerical data allow one to analyze the frequency crossover for the GH shift. They show an excellent agreement with our analytical predictions. The data also show that the maximum GH shift is near to the critical angle [34]. Thus, experiments in this region represent the most favorable situation to investigate this shift.

In a forthcoming paper, we aim to analyze in detail the behavior of gaussian optical beams incident at critical angles in the case in which the outgoing wave number distribution is asymmetric.

Acknowledgements

We gratefully thank the referee for his useful suggestions and for drawing our attention to the references [25,26].

Funding

We gratefully thank the Capes (M.P.A.), Fapesp (S.A.C.), and CNPq (S.D.L.) for financial support.

References

[1] Baida, F.I.; Labeke, D.V.; Vigoureux, J.M. *J. Opt. Soc. Am. A* **2000**, *17*, 858–866.
[2] Broe, J.; Keller, O. *J. Opt. Soc. Am. A* **2002**, *19*, 1212–1222.
[3] Seshadri, S.R. *J. Opt. Soc. Am. A* **1988**, *5*, 583–585.
[4] Yasumoto, K.; Oishi, Y. *J. Appl. Phys.* **1983**, *54*, 2170–2176.
[5] Liu, X.; Yang, Q. *J. Opt. Soc. Am. B* **2010**, *27*, 2190–2194.
[6] Prajapati, C.; Ranganathan, D. *J. Opt. Soc. Am. A* **2012**, *29*, 1377–1382.
[7] Aiello, A. *New J. Phys.* **2012**, *14*, 013058–12.
[8] Wan, Y.; Zheng, Z.; Kong, W.; Zhao, X.; Liu, Y.; Bian, Y.; Liu, J. *Opt. Express* **2012**, *20*, 8998–9003.
[9] Dennis, M.R.; Götte, J.B. *New J. Phys.* **2012**, *14*, 073013–13.
[10] McGuirk, M.; Carniglia, C.K. *J. Opt. Soc. Am.* **1977**, *67*, 103–107.
[11] Bliokh, K.Y.; Aiello, A. *J. Opt.* **2013**, *15*, 014001–16.
[12] Götte, J.B.; Shinohara, S.; Hentschel, M. *J. Opt.* **2013**, *15*, 014009–8.
[13] Newton, I., Sir *Opticks: or, a Treatise of the Reflections, Refractions, Inflections and Colours of Light;* Printed for William Innys at the West End of St. Paul's: London, 1730.
[14] Picht, J. *Ann. Phys. (Berlin, Ger.)* **1925**, *382*, 785–882.
[15] Schaefer, C.; Pich, R. *Ann. Phys. (Berlin, Ger.)* **1937**, *422*, 245–266.
[16] Goos, F.; Hänchen, H. *Ann. Phys. (Berlin, Ger.)* **1947**, *436*, 333–346.
[17] Artmann, K. *Ann. Phys. (Leipizig, Ger.)* **1948**, *437*, 87–102.
[18] Fragstein, C.v. *Ann. Phys. (Berlin, Ger.)* **1949**, *439*, 271–278.
[19] Cowan, J.J.; Anicin, B. *J. Opt. Soc. Am.* **1977**, *67*, 1307–1314.
[20] Ghatak, A.K.; Shenoy, M.R.; Goyal, I.C.; Thyagarajan, K. *Opt. Commun.* **1986**, *56*, 313–317.
[21] Haibel, A.; Nimtz, G.; Stahlhofen, A.A. *Phys. Rev. E* **2001**, *63*, 047601–3.
[22] Li, C.F. *Phys. Rev. Lett.* **2003**, *91*, 133903–3.
[23] Briers, R.; Leroy, O.; Shkerdin, G. *J. Acoust. Soc. Am.* **2000**, *108*, 1622–1630.
[24] Emile, O.; Galstyan, T.; Le Floch, A.; Bretenaker, F. *Phys. Rev. Lett.* **1995**, *75*, 1511–1513.
[25] Birman, J.L.; Pattanayak, D.N.; Puri, A. *Phys. Rev. Lett.* **1983**, *50*, 1664–1667.
[26] Puri, A.; Pattanayak, D.N.; Birman, J.L. *Phys. Rev. B* **1983**, *28*, 5877–5886.
[27] Harrick, N.J. *Phys. Rev. Lett.* **1960**, *4*, 224–226.
[28] Yin, X.; Hesselink, L. *Appl. Phys. Lett.* **2006**, *89*, 261108–5.
[29] Yu, T.; Li, H.; Cao, Z.; Wang, Y.; Shen, Q.; He, Y. *Opt. Lett.* **2008**, *33*, 1001–1003.
[30] Sakata, T.; Togo, H.; Shimokawa, F. *Appl. Phys. Lett.* **2000**, *76*, 2841–2841.
[31] Chen, L.; Cao, Z.Q.; Ou, F.; Li, H.G.; Shen, Q.S.; Qiao, H.C. *Opt. Lett.* **2007**, *32*, 1432–1434.
[32] Pflegaar, E.; Marseille, A.; Weis, A. *Phys. Rev. Lett.* **1993**, *70*, 2281–2284.
[33] Qin, Y.; Li, Y.; Feng, X.; Xiao, Y.F.; Yang, H.; Gong, Q. *Opt. Express* **2011**, *19*, 9636–9645.
[34] Lai, H.M.; Cheng, F.C.; Tang, W.K. *J. Opt. Soc. Am. A* **1986**, *3*, 550–557.
[35] Nasalski, W.; Tamir, T.; Lin, L. *J. Opt. Soc. Am. A* **1988**, *5*, 132–140.
[36] Horowitz, B.R.; Tamir, T. *J. Opt. Soc. Am.* **1971**, *61*, 586–594.
[37] De Leo, S.; Rotelli, P. *Eur. Phys. J. D* **2011**, *61*, 481–488.
[38] De Leo, S.; Rotelli, P. *Eur. Phys. J. D* **2011**, *65*, 563–570.
[39] Wigner, E. *Phys. Rev.* **1955**, *98*, 145–147.

[40] Bleistein, N.; Handelsman, R. *Asymptotic Expansions of Integrals*; Dover: New York, 1975.
[41] De Leo, S.; Rotelli, P. *J. Opt. A: Pure Appl. Opt.* **2008**, *10*, 115001–5.
[42] Born, M.; Wolf, E. *Principles of Optics*; Cambridge University Press: Cambridge, UK, 1999.
[43] Saleh, B.E.A.; Teich, M.C. *Fundamentals of Photonics*; Wiley: New Jersey, 2007.